

Rearrangement of electron shells and interchannel interaction in the K photoabsorption of Ne

N. M. Novikovskiy¹, D. V. Rezvan¹, N. M. Ivanov¹, I. D. Petrov², B. M. Lagutin²
A. Knie³, A. Ehresmann³, Ph. V. Demekhin³, and V. L. Sukhorukov^{1,3}

¹ Institute of Physics, Southern Federal University, 344090 Rostov-on-Don, Russia

² Rostov State Transport University, 344038 Rostov-on-Don, Russia

³ Institute of Physics and Center for Interdisciplinary Nanostructure Science and Technology (CINSaT), University of Kassel, D-34132, Kassel, Germany

Received: date / Revised version: date

Abstract. A detailed theoretical analysis of the $1s$ photoionization of neon is presented. It is found that the most significant many-electron correlation in computing photoionization of inner shells is the rearrangement of the outer shells caused by the inner vacancy. Further noticeable effects are: (i) the polarization of the ion core by the outgoing photoelectron and (ii) the coherent effect of double excitation/ionization. The core polarization increases the photoionization cross section by about 10% at the $1s$ threshold, and the coherent excitation results in further increases by about 5%. Incoherent excitation of the satellite channel leads to an additional 10% increase in the photoabsorption cross section in the double-ionization threshold region.

PACS. 32.80.Fb Photoionization of atoms and ions – 32.80.Aa Inner-shell excitation and ionization – 31.15.V Electron correlation calculations for atoms, ions and molecules

1 Introduction

Recently, the interest in studying the photoabsorption by electrons of inner atomic shells has been renewed as this process has been used to study the interstellar medium (see, e.g., [1,2] and references therein). Despite the fact that photoabsorption of inner atomic shells has been studied for more than half a century, there are still noticeable discrepancies between the various theoretical [3,4,5,6] and experimental [2,7,8] spectra even in case of the prototypical neon.

Photoabsorption cross section $\sigma_{1s}^{Abs}(\omega)$ of Ne as function of the exciting-photon energy has been measured more than 50 years ago [9]. The experimental resolution in that work was sufficient to observe spectral features associated with Rydberg series whereas the $\sigma_{1s}^{Abs}(\omega)$ cross section has been determined on an arbitrary scale. The absolute photoionization cross section for the $1s$ shell of Ne has been computed in [3] considering the rearrangement of atomic shells by the $1s$ vacancy. Using the synchrotron radiation allowed Esteva et al. [7] to obtain cross section $\sigma_{1s}^{Abs}(\omega)$ on an absolute scale and to reveal some additional above-threshold sharp spectral features which have been interpreted as shake satellites connected mainly with the $1s^{-1}2p^{-1}3p^2\ ^1P$ terms. The cross sections for production of those satellites have been calculated in our earlier paper

[10] with taking into account the doubly-excited states. It was revealed that the satellites observed in [7] in addition to the $1s^{-1}2p^{-1}3p^2\ ^1P$ terms are also determined by the states of the $1s^{-1}2p^{-1}3p4p$ configurations and by the strong many-electron correlation known as the dipole polarization of electron shells (DPES) [11] which is described mainly by the $3p3p - 3s(n/\varepsilon)(s/d)$ excitations. In paper [10] it was also mentioned that an interaction between the autoionizing doubly-excited states and respective continua can result in Fano-type [12] resonance profiles. These resonances are energetically located starting from about 30 eV above the $1s$ - threshold. Therefore, the precise theoretical description of those resonances can be separated from the problem of computing the smooth cross section in the energy region just above the $1s$ threshold.

Kutzner and Rose [5] modified the relativistic random-phase approximation to include the rearrangement of the ionic core and computed the Ne $\sigma_{1s}^{Abs}(\omega)$ cross section adding the background from the photoionization of the $2s$ and $2p$ shells. Gorczyca [6] applied the R-matrix MQDT optical potential method in order to compute the photoabsorption cross section in the region of the $1s^{-1}np$ resonances and just above the $1s$ threshold.

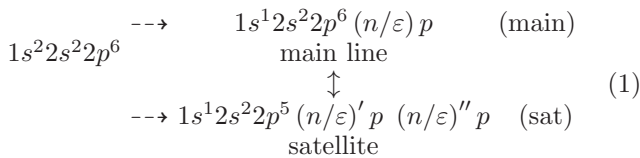
An absolute Ne $\sigma_{1s}^{Abs}(\omega)$ cross section has been determined anew by Suzuki and Saito [8] using monochromatized synchrotron radiation in the extended energy range between 50–1300 eV, but with broad bandwidth. The ab-

solute threshold photoabsorption cross section $\sigma_{1s}^{Abs}(\omega_{thr})$ was about 10% smaller than previously measured by Esteve et al. [7]. Near-threshold photoabsorption cross section $\sigma_{1s}^{Abs}(\omega)$ of Ne has been measured by Prince et al. [12] with high resolution. This experiment revealed that the doubly-excited shake resonances have the asymmetric Fano shape as predicted in [10] but resulted in the threshold cross section $\sigma_{1s}^{Abs}(\omega_{thr}) = 0.45$ Mb which is substantially larger than that measured by Suzuki and Saito [8] $\sigma_{1s}^{Abs}(\omega_{thr}) = 0.376$ Mb. The reason of this observation is not completely clear but supposedly it can be connected with overestimated photoabsorption by the $2s$ and $2p$ shells obtained in [12]. Indeed, the value of this cross section $\sigma_{2s+2p}(\omega_{thr}) = 0.09$ Mb measured in [12] is about 4 times larger than that reported in [8] $\sigma_{2s+2p}(\omega_{thr}) = 0.0228$ Mb. High-resolution near-threshold $1s$ photoabsorption cross section has been determined by Müller et al. [2]. Both experiments [2,8] yield cross sections which are smaller by about 10% in the threshold region than that measured previously [7]. A similar difference exists between the calculations [3,6] and [5].

In the present study, we calculate the Ne $\sigma_{1s}^{Abs}(\omega)$ cross section with ‘step-by-step’ inclusion of different many-electron correlations concentrating on the ‘smooth’ region which is free of the doubly-excited resonances. This procedure allows to clarify the individual role of each many-electron correlation in the photoionization of inner shells.

2 Method of calculation

Photoabsorption of Ne near the $1s$ threshold is determined mainly by the channels shown in scheme (1). Background absorption stems from the $2s \rightarrow \varepsilon p$ and $2p \rightarrow \varepsilon\{s, d\}$ photoionization. The latter processes produce photoelectrons with large energies at the $1s$ threshold and, therefore, are not strongly affected by many-electron correlations in this exciting-photon energy range. Contrary, processes (1) release photoelectrons with small energies, which results in a substantial influence of many-electron correlations on the cross sections of channels (1main) and (1sat):



Transition amplitudes are composed of the direct \mathbf{D} and correlational \mathbf{D}^{corr} parts:

$$A_{1s}^{\varepsilon p} = \langle 1s^1 2s^2 2p^6 \varepsilon p | \mathbf{D} + \mathbf{D}^{\text{corr}} | 1s^2 2s^2 2p^6 \rangle \quad (2)$$

where

$$\langle 1s^1 2s^2 2p^6 \varepsilon p | \mathbf{D} | 1s^2 2s^2 2p^6 \rangle = \sqrt{2} \langle \varepsilon p | \mathbf{d} | 1s \rangle \quad (3)$$

and

$$\langle 1s^1 2s^2 2p^6 \varepsilon p | \mathbf{D}^{\text{corr}} | 1s^2 2s^2 2p^6 \rangle = \sqrt{2} \times \sum_{\varepsilon', \varepsilon''} \frac{(6F^0 - G^0 - 0.4G^2) \langle \varepsilon' p | 2p \rangle \langle \varepsilon'' p | \mathbf{d} | 1s \rangle}{IP(1s^{-1}) + \varepsilon - IP(1s^{-1} 2p^{-1}) - \varepsilon' - \varepsilon'' + i\delta}. \quad (4)$$

In equation (4), IP denotes the ionization potential of the respective state; the sum over ε' and ε'' includes summation over the discrete and integration over the continuum states; the notations $F^0 \equiv R^0(2p\varepsilon p; \varepsilon' p \varepsilon'' p)$ and $G^k \equiv R^k(2p\varepsilon p; \varepsilon'' p \varepsilon' p)$ for the Slater integrals are used for brevity.

The one-electron matrix elements of the electric dipole transition operator, \mathbf{d} , entering equations (3), (4) are given by [3,10]:

$$\begin{aligned} \langle \varepsilon p | \mathbf{d} | 1s \rangle &= \langle 1s^+ | 1s \rangle \langle 2s^+ | 2s \rangle^2 \langle 2p^+ | 2p \rangle^6 \\ &\times \left[\langle \varepsilon p^+ | \mathbf{d} | 1s \rangle - \langle 2p^+ | \mathbf{d} | 1s \rangle \frac{\langle \varepsilon p^+ | 2p \rangle}{\langle 2p^+ | 2p \rangle} \right. \\ &\quad \left. - \langle \varepsilon p^+ | \mathbf{d} | 2s \rangle \frac{\langle 2s^+ | 1s \rangle}{\langle 2s^+ | 2s \rangle} \right], \quad (5) \end{aligned}$$

where $\langle \text{bra}^+ |$ and $| \text{ket} \rangle$ AOs are computed in configurations $1s^1 2s^2 2p^6$ and $1s^2 2s^2 2p^6$, respectively; $\langle n' \ell' | \mathbf{d} | n \ell \rangle$ is the radial integral computed either in length or in velocity gauges, depending on the sign in equation (6). The transition amplitude (2) determines the photoionization cross section of the $1s \rightarrow \varepsilon p$ transition as:

$$\sigma_{1s}(\omega) = \frac{4}{3} \pi^2 \alpha a_0^2 \omega^{\pm 1} |A_{1s}^{\varepsilon p}|^2, \quad (6)$$

where the signs (+) and (−) correspond to the length and velocity forms of operator \mathbf{d} , respectively; ω denotes the exciting photon energy in atomic units; $\alpha = 1/137.036$ is the fine structure constant; the square of the Bohr radius $a_0^2 = 28.0028$ Mb converts atomic units for cross sections to Mb = 10^{-22} m². The exciting photon energy ω and the photoelectron energy, ε , counted from the $1s$ threshold, $IP(1s^{-1})$, are related via:

$$\omega = IP(1s^{-1}) + \varepsilon. \quad (7)$$

The values of terms in square brackets for the transition amplitude (5) are depicted as functions of electron energy in Fig. 1. The transition amplitude computed in the frozen core approximation FC is shown in the same figure for comparison. One can recognize that the relaxation of the ionic core strongly decreases the amplitude $\langle \varepsilon p | \mathbf{d} | 1s \rangle$ computed within the FC approach whereas additional terms compensate this decrease at $\varepsilon \leq 150$ eV. It is important to note that the application of the theory of non-orthogonal orbitals implies the orthogonality of the total wave function of an ionic state to the all low-lying state wave functions. In the considered case of Ne it means that the total wave function for the configuration $1s^1 2s^2 2p^6$ should be orthogonal to the $1s^2 2s^1 2p^6$ one. The

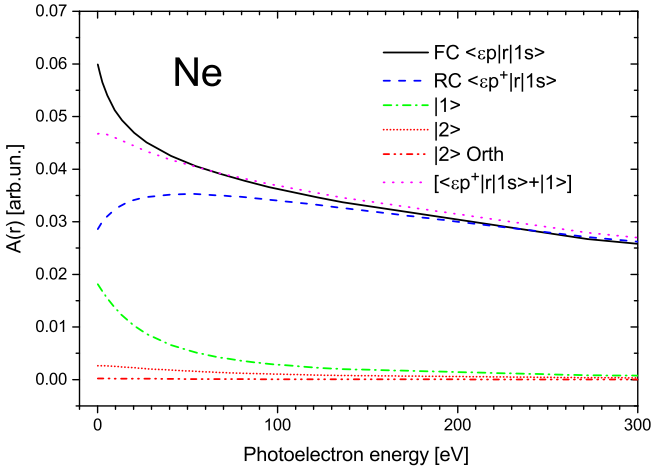


Fig. 1. Comparison between partial transition amplitudes computed within the frozen core approach (FC), different terms contained in square brackets of equation (5), and the sum of these terms. Dash-double dotted and dotted curves show the 3rd term in square brackets of (5) computed with and without taking into account orthogonality condition, respectively (see text).

fulfilment of this requirement results in a decrease of the 3rd term in square brackets of equation (5) by about one order of magnitude (cf. short dotted and dash-double dotted curves in Fig. 1), allowing to neglect these terms in the calculations.

The photoionization cross section for the satellite production (pathway (1sat)) was calculated via the following equation adopted from Refs. [10,13] for the case of the $1s2p \rightarrow (n/\varepsilon)'p(n/\varepsilon)''p$ transition in Ne:

$$\sigma_{1s2p}(\omega) = \frac{4\pi^2\alpha a_0^2}{3} \frac{12\omega}{1 + \delta_{n'n''}} \int_0^{\omega - IP(1s^{-1}2p^{-1})} [A^2 + B^2 - AB/3] d\varepsilon'', \quad (8)$$

where

$$\begin{aligned} A &= \langle (n/\varepsilon)'p | d | 1s \rangle \langle (n/\varepsilon)''p | 2p \rangle, \\ B &= \langle (n/\varepsilon)''p | d | 1s \rangle \langle (n/\varepsilon)'p | 2p \rangle, \end{aligned} \quad (9)$$

and integration over ε'' is carried out over the following surface:

$$\omega = IP(1s^{-1}2p^{-1}) + \varepsilon' + \varepsilon'', \quad \varepsilon' \leq \varepsilon''. \quad (10)$$

If either photoelectron or excited electron belongs to a discrete $n'p$ state, the integration over the ε'' in equation (8) is lifted, and ε'' is determined as:

$$\omega = IP(1s^{-1}2p^{-1}n'p) + \varepsilon''. \quad (11)$$

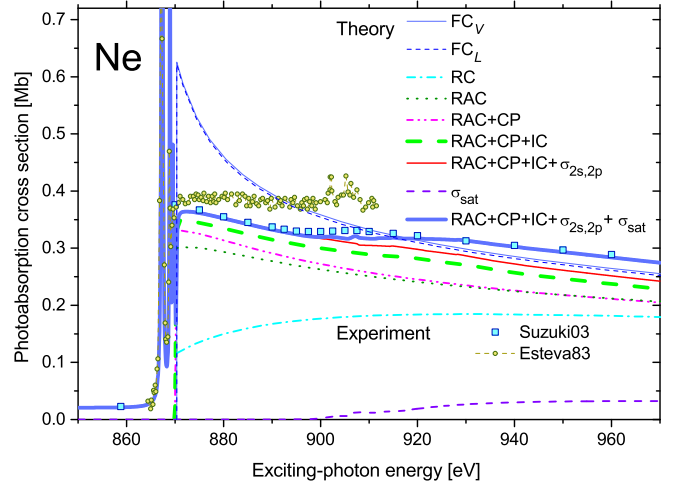


Fig. 2. Photoionization cross sections $\sigma_{1s}(\omega)$ computed in the approximations described in the text. The lowest dashed curve shows the cross section for the satellite production $\sigma_{1s2p}(\omega)$. The thick solid line represents the computed photoabsorption cross section $\sigma_{1s}^{Abs}(\omega)$. Experimental photoabsorption data ‘Estevea83’ and ‘Suzuki03’ are from Refs. [7] and [8], respectively. The size of points representing experiment [8] corresponds to error bars claimed in this work.

3 Results and discussion

In order to clarify the influence of different many-electron correlations on the inner-shell photoionization we computed cross section $\sigma_{1s}^{\varepsilon p}(\omega)$ of Ne in different approximations:

FC Frozen core approach, where the relaxation of atomic orbitals (AOs) by the $1s$ vacancy was neglected. The core orbitals were obtained in the neutral ground configuration $1s^22s^22p^6$, and were also used to compute the AO of the photoelectron in the $1s^12s^22p^6\varepsilon p^1P$ state.

RC Relaxed core approach, which takes into account the relaxation of AOs. The core AOs of the initial state were taken from the FC approach; for the final state core AOs $P_{n\ell}^+(r)$ were computed in the self-consistent configuration $1s^12s^22p^6$; the photoelectron AOs $P_{\varepsilon p}^+(r)$ were computed in the ‘relaxed’ core AOs.

RAC Rearranged core approach, where additional second term enters the transition amplitude (5).

RAC+CP *Ab initio* core polarization potential [14] was included into the equation for the photoelectron AOs $P_{\varepsilon p}^+(r)$ in addition to the RAC approach.

RAC+CP+IC The coherent correlational part of the transition amplitude \mathbf{D}^{corr} (4) caused by the interaction between the ‘satellite’ $1s2p - \varepsilon'p\varepsilon''p$ and the ‘main’ $1s - \varepsilon p$ channels was taken into account in addition to the approximations discussed above.

Photoionization cross sections $\sigma_{1s}(\omega)$ computed in the described approximations are depicted in Fig. 2. Velocity gauge is used for presentation, because length and velocity results agree fairly well (cf. cross sections FC_L and FC_V computed in the length and velocity gauges, respectively).

In order to simplify the figure, the below-threshold region is shown only for the final result (thick solid line).

In Fig. 2, we set the computed $1s$ threshold to the measured experimental value $IP_{Exp}(1s^{-1}) = 870.33$ eV, which was estimated by us using the Rydberg formula and the data of Ref. [2]. The estimated value agrees with the value recommended by NIST, $IP_{Exp}(1s^{-1}) = 870.23(18)$ eV [15], within the error bar. In the present work, the value of the $1s$ threshold was computed within the Pauli-Fock approximation, which uses the Breit operator for description of the relativistic corrections [16]. The computed value of $IP_{PF}(1s^{-1}) = 869.55$ eV, is by 0.78 eV smaller than the measured one because of neglecting high-order corrections of perturbation theory to the total energies of the $1s^2 2s^2 2p^6$ and $1s^1 2s^2 2p^6$ configurations.

From Fig. 2, one can see that the frozen core approximation FC overestimates the cross section at the $1s$ threshold $\sigma_{1s}(\omega_{thr})$. Taking into account the core relaxation (RC approach) decreases $\sigma_{1s}(\omega_{thr})$ by a factor of 5.6. The additional term in equation (5) (RAC approach) increases $\sigma_{1s}(\omega_{thr})$ by a factor of 2.7, thus partly compensating the previous decrease. The further increase of the $\sigma_{1s}(\omega_{thr})$ by about 10% stems from taking into account the core polarization potential. The increase of $\sigma_{1s}(\omega_{thr})$ due to the coherent pathway (1sat) is twice smaller than due to core polarization but results in the appearance of two inflection points in the $\sigma_{1s}(\omega)$ curve at $\omega = 913.0$ eV and $\omega = 934.5$ eV. It is very desirable to confirm the existence of these points experimentally applying, e.g., photoelectron spectroscopy.

In order to obtain the photoabsorption cross section $\sigma_{1s}^{Abs}(\omega)$, the photoionization cross sections of the outer shells $\sigma_{2s}(\omega)$, $\sigma_{2p}(\omega)$ and the cross section for the satellites production $\sigma_{1s2p}(\omega)$ (8) were computed. It turned out that intrashell and intershell correlations [17] have small influence on $\sigma_{2s}(\omega)$ and $\sigma_{2p}(\omega)$ because of the large photoelectron energy ε at the $1s$ threshold. The absolute values of $\sigma_{2s}(\omega_{thr}) = 0.014$ Mb and $\sigma_{2p}(\omega_{thr}) = 0.005$ Mb at the $1s$ threshold are small compared to the $\sigma_{1s}(\omega_{thr}) = 0.364$ Mb. The resulting value of $\sigma_{2s+2p}(\omega_{thr}) = 0.019$ Mb is slightly less than the background value of $\sigma_{2s+2p}(\omega_{thr}) = 0.0228$ Mb determined experimentally [8].

The cross section for the satellites production $\sigma_{1s2p}(\omega)$ computed according to equation (8) is presented by the lowest dashed curve in Fig. 2. Precise calculation of the lineshapes produced by the autoionizing doubly-excited $1s^1 2p^5 nln'l'$ resonances is a separate cumbersome problem (see, e.g. [18]) which is out of scope of the present paper. Therefore, we computed the integral cross section for the production of the $1s2p - npn'p$ satellites via equation (8) and presented them by Gaussians with FWHM of 1.6 eV located at the center of gravity of the respective $1s^1 2p^5 npn'p$ configuration. This Gaussian FWHM was obtained using the transition array technique [19,20]. This technique simulates the multiplet splitting of the configurations with many open shells and it is known to be very effective in the overall description of complicated atomic spectra [21].

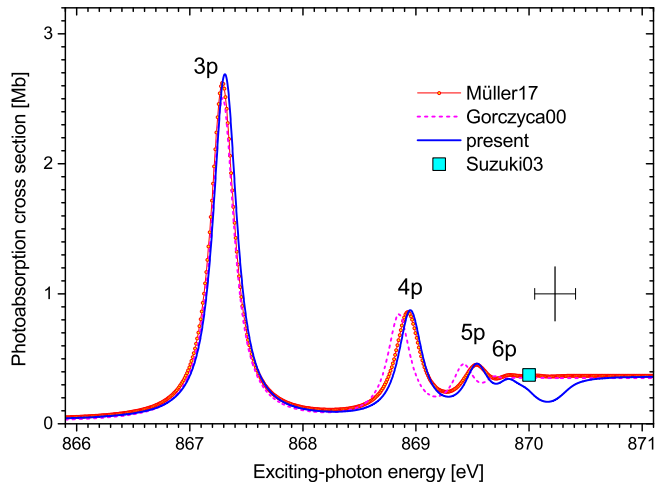


Fig. 3. Comparison between the photoabsorption cross section $\sigma_{1s}^{Abs}(\omega)$ computed in the present work, in the work of Gorczyca [6] and experimentally determined by Müller et al. [2]. A single experimental point obtained by Suzuki and Saito [8] falling in the depicted energy interval is also shown. The energy scale of Gorczyca [6] was set to the experimental scale of Ref. [2] using the first peak related with the $1s \rightarrow 3p$ transition, whereas our energy scale was set to the experimental one using the $1s$ threshold (see text).

In Fig. 2, the resulting photoabsorption cross section is denoted as ‘**RAC + CP + IC** + $\sigma_{2s,2p}(\omega) + \sigma_{sat}(\omega)$ ’. One can see that the presently computed cross section $\sigma_{1s}^{Abs}(\omega)$ is in excellent agreement with the data of Suzuki and Saito [8], whereas it differs from $\sigma_{1s}^{Abs}(\omega)$ measured by Esteve et al. [7]. It could be of great interest to clarify the reason of this disagreement.

The computed below-threshold photoabsorption cross sections are presented in an enlarged scale in Fig. 3 by the thick solid curve. The minimum in presently computed $\sigma_{1s}^{Abs}(\omega)$ at ω about 870.2 eV stems from considering the $1s^{-1}np$ ($n = 3 - 7$) resonances only, whereas the experiment includes the infinite np Rydberg series. Lines corresponding to the $1s - np$ transitions are convolved with Lorentzians of FWHM 0.230 eV and with their area computed as:

$$f_{\sigma}(1s - np) [\text{Mb} \cdot \text{eV}] = 2\pi^2 \alpha a_0^2 \cdot f(1s - np) \cdot 2\text{Ry}[\text{eV}], \quad (12)$$

where f is the dimensionless oscillator strength of the $1s - np$ transition converted to the area under the $\sigma_{1s}(\omega)$ curve (or ‘dimensioned’ oscillator strength f_{σ} which has a meaning of the photoionization cross section) by multiplying with a factor $2\pi^2 \alpha a_0^2 \cdot 2\text{Ry}$. The FWHM was taken equal to the natural width of the $1s$ level Γ_{1s} , which was computed in the present work using the self-consistent AOs of the $1s^1 2s^2 2p^6$ configuration. This approximation is known to result in adequate values of natural widths [22]. $\Gamma_{1s} = 0.230$ eV agrees well with $\Gamma_{1s} = 0.241$ eV computed in [6] and is slightly smaller than the experimental value $\Gamma_{1s} = 0.271(20)$ eV [4].

Table 1. Oscillator strengths $f_\sigma(1s - np)$ (12) computed for Ne in different approximations.

np	Approximation					Exp. [2] ^c
	FC	RC	RAC	+CP ^a	+IC ^b	
3p	3.513	0.281	0.827	0.964	1.010	1.027
4p	0.733	0.094	0.258	0.294	0.308	0.307
5p	0.287	0.042	0.113	0.127	0.134	

^a Approximation **RAC+CP** (see text)^b Approximation **RAC+CP+IC**^c Values are estimated by us (see text)

In Fig. 3, the $\sigma_{1s}^{Abs}(\omega)$ computed below the ionization threshold is compared with theoretical data of Gorczyca [6] and experimental data of Müller et al. [2] in an enlarged scale. Small differences between energy positions of the $1s^{-1}np$ resonances and their oscillator strengths f_σ computed in [6] and measured in [2] could be connected with neglecting the core polarization in those calculations [6]. An excellent agreement between our calculation and experiment [2] is evident from Fig 3.

Oscillator strengths $f_\sigma(1s - np)$ (12) computed in the different approximations are listed in Table 1 in comparison to experimental data. Experimental values were obtained by fitting cross sections with a constant background (appeared to be 0.025(1) Mb) and Lorentzians. One can see that the general trends in the computed cross sections between different approximations is similar to that for the photon energies above the ionization threshold, but they become more pronounced. For instance, the relaxation of the core under the $1s$ vacancy resulted in a decrease of $f_\sigma(1s - 3p)$ by a factor of 12.5 with subsequent compensation due to additional terms by a factor of 2.9. Taking into account of the core polarization increases $f_\sigma(1s - 3p)$ by about 17%. An excellent agreement between the final result obtained in the present work and the experimental value from [2] can be seen from the last two columns of Table 1.

4 Conclusions

The absolute photoabsorption cross sections as a function of the exciting-photon energy $\sigma_{1s}^{Abs}(\omega)$ was calculated for Ne with taking into account important many electron correlation effects. To solve this problem we computed photoionization cross sections $\sigma_{1s}(\omega)$, $\sigma_{2s}(\omega)$, $\sigma_{2p}(\omega)$ and the cross section $\sigma_{1s2p}(\omega)$ for the satellite production. The influence of different many-electron correlations on the computed $\sigma_{1s}(\omega)$ was investigated in details. The following many-electron correlation are important in describing the near-threshold photoabsorption of the Ne $1s$ shell (in decreasing order): (i) relaxation of the core atomic orbitals caused by the $1s$ vacancy; (ii) rearrangement of the transition amplitude caused by the relaxation of atomic orbitals; (iii) polarization of the core by the outgoing (or excited) electron; (iv) coherent interaction between main

and satellite photoionization channels. Excellent agreement between the present theory and recent experiment allows to conclude the adequacy of the approximation used here for the description of the inner-shell photoionization. Coherent interaction between the main and satellite channels results in the appearance of two inflection points in the $\sigma_{1s}(\omega)$ photoionization function in the region of the double-ionization threshold. It could be interesting to check this prediction experimentally.

5 Authors contributions

VLS conceived the idea and coordinated the research project; PhVD designed, produced and tested computer programs; NMN, IDP, DVR, NMI performed the calculations and combined the results; BML, AK, AE participated in discussion of results and contributed to writing manuscript. All authors were involved in the preparation of the manuscript, commented and approved its final version.

This work was partly supported by the Deutsche Forschungsgemeinschaft (DFG) within the Sonderforschungsbereich SFB-1319 ‘Extreme Light for Sensing and Driving Molecular Chirality – ELCH’. NMN, IDP, BML and VLS would like to thank the Institute of Physics, University of Kassel for the hospitality. VLS appreciate support from Southern Federal University within the inner project no 3.6105.2017/BP. IDP and BML appreciate support from the grant no 16-02-00771a of the RFBR. We are grateful to Prof. A. Müller and Prof. T.W. Gorczyca for providing in digital form data from papers [2] and [6], respectively.

References

1. E. Gatuzz, J. García, T.R. Kallman, C. Mendoza, T.W. Gorczyca, *Astrophys. J.* **800**, 29 (2015)
2. A. Müller, D. Bernhardt, A.B. Jr., T. Buhr, J. Hellhund, K. Holste, A.L.D. Kilcoyne, S. Klumpp, M. Martins, S. Ricz et al., *Astrophys. J.* **836**, 166 (2017)
3. V.L. Sukhorukov, V.F. Demekhin, V.V. Timoshevskaya, S.V. Lavrentev, *Opt. Spectrosc. (USSR)* **47**, 407 (1979)
4. M. Coreno, L. Avaldi, R. Camilloni, K.C. Prince, M. de Simone, J. Karvonen, R. Colle, S. Simonucci, *Phys. Rev. A* **59**, 2494 (1999)
5. M. Kutzner, M. Rose, *J. Phys. B: At., Mol. Opt. Phys.* **32**, 123 (1999)
6. T.W. Gorczyca, *Phys. Rev. A* **61**, 024702 (2000)
7. J.M. Esteva, B. Gauthe, P. Dhez, R.C. Karnatak, *J. Phys. B: At. Mol. Phys.* **16**, L263 (1983)
8. I.H. Suzuki, N. Saito, *J. Electron Spectrosc. Relat. Phenom.* **129**, 71 (2003)
9. R.J. Liefeld, *Appl. Phys. Lett.* **7**, 276 (1965)
10. V.L. Sukhorukov, A.N. Hopersky, I.D. Petrov, V.A. Yavna, V.F. Demekhin, *J. de Phys.* **48**, 1677 (1987)
11. V. Sukhorukov, I. Petrov, B. Lagutin, A. Ehresmann, K.H. Schartner, H. Schmoranzner, *Phys. Rep.* (2018), <https://doi.10.1016/j.physrep.2018.10.004>

12. K. Prince, L. Avaldi, R. Sankari, R. Richter, M. de Simone, M. Coreno, J. Electron Spectrosc. Relat. Phenom. **144**, 43 (2005), proceeding of the Fourteenth International Conference on Vacuum Ultraviolet Radiation Physics
13. V.L. Sukhorukov, A.N. Hopersky, I.D. Petrov, J. de Phys. II **1**, 501 (1991)
14. I.D. Petrov, V.L. Sukhorukov, H. Hotop, J. Phys. B: At. Mol. Opt. Phys. **32**, 973 (1999)
15. R. Deslattes, E. Kessler Jr., P. Indelicato, and NIST X-ray-Trans Team, *X-ray Transition Energies (version 1.2)*. [Online] (National Institute of Standards and Technology, Gaithersburg, MD, 2005), DOI:10.18434/T4859Z
16. R. Kau, I.D. Petrov, V.L. Sukhorukov, H. Hotop, Z. Phys. D **39**, 267 (1997)
17. M.Y. Amusia, *Atomic Photoeffect*, 1st edn. (Plenum Press, New York, 1990), ISBN 0-306-43548-9
18. V.L. Sukhorukov, I.D. Petrov, M. Schäfer, F. Merkt, M.W. Ruf, H. Hotop, J. Phys. B: At., Mol. Opt. Phys. **45**, 092001 (2012), topical Review
19. C. Bauche-Arnoult, J. Bauche, M. Klapisch, Phys. Rev. A **20**, 2424 (1979)
20. C. Bauche-Arnoult, J. Bauche, M. Klapisch, Phys. Rev. A **25**, 2641 (1982)
21. J. Bauche, C. Bauche-Arnoult, M. Klapisch, Adv. At. Mol. Phys. **23**, 131 (1988)
22. G. Howat, J. Phys. B: At. Mol. Phys. **11**, 1589 (1978)